European Journal of Neuroscience, Vol. 20, pp. 729–739, 2004

Kv3 K^+ channels enable burst output in rat cerebellar Purkinje cells

B. E. McKay and R. W. Turner
Neuroscience Research Group, University of Calgary, Calgary, Alberta, Canada T2N 4 N1

Keywords: burst discharge, calcium spike, dendritic spike, Kv3 potassium channels, repolarization

Abstract

The ability of cells to generate an appropriate spike output depends on a balance between membrane depolarizations and the repolarizing actions of K^+ currents. The high-voltage-activated Kv3 class of K^+ channels repolarizes Na^+ spikes to maintain high frequencies of discharge. However, little is known of the ability for these K^+ channels to shape Ca^{2+} spike discharge or their ability to regulate Ca^{2+} spike-dependent burst output. Here we identify the role of Kv3 K^+ channels in the regulation of Na^+ and Ca^{2+} spike discharge, as well as burst output, using somatic and dendritic recordings in rat cerebellar Purkinje cells. Kv3 currents pharmacologically isolated in outside-out somatic membrane patches accounted for $\sim$40% of the total K^+ current, were very fast and high voltage activating, and required more than 1 s to fully inactivate. Kv3 currents were differentiated from other tetraethylammonium-sensitive currents to establish their role in Purkinje cells under physiological conditions with current-clamp recordings. Dual somatic-dendritic recordings indicated that Kv3 channels repolarize Na^+ and Ca^{2+} spikes, enabling high-frequency discharge for both types of cell output. We further show that during burst output Kv3 channels act together with large-conductance Ca^{2+}-activated K^+ channels to ensure an effective coupling between Ca^{2+} and Na^+ spike discharge by preventing Na^+ spike inactivation. By contributing significantly to the repolarization of Na^+ and especially Ca^{2+} spikes, our data reveal a novel function for Kv3 K^+ channels in the maintenance of high-frequency burst output for cerebellar Purkinje cells.

Introduction

The Kv3 class of K^+ channels (Kv3.1–3.4) exhibits a high voltage for activation and fast rate of deactivation, making them excellent candidates for repolarizing Na^+ spikes and generating fast AHPs (Rudy & McBain, 2001). The Kv3.1 and 3.2 subtypes are often co-expressed at high density in somatic and axonal membranes of cells that discharge spikes at high frequencies, supporting a role in maintaining repetitive Na^+ spike discharge (Sekirnjak *et al*., 1997; Martina *et al*., 1998; Wang *et al*., 1998b; Erisir *et al*., 1999; Devaux *et al*., 2003; Fernandez *et al*., 2003; Lien & Jonas, 2003). Kv3.3 K^+ channels have been shown to extend over the entire soma-dendritic axis of electrosensory pyramidal cells, where repolarization of somatic and dendritic Na^+ spikes regulates the threshold for burst discharge (Rashid *et al*., 2001a,b; Noonan *et al*., 2003). Cerebellar Purkinje cells express both Kv3.3 and Kv3.4 K^+ channels; expression of Kv3.1 is negligible and Kv3.2 subunits are absent (Goldman-Wohl *et al*., 1994; Weiser *et al*., 1994; Rashid *et al*., 2001a; Martina *et al*., 2003). For these cells, a different spatial distribution of Na^+ and Ca^{2+} spike discharge provides even greater potential for Kv3 channels to regulate spike output. After a Na^+ spike initiates in the Purkinje cell axon it propagates actively into the soma and conducts in a primarily passive manner over the proximal dendritic region (Llinas & Sugimori, 1980a,b; Stuart & Hausser, 1994; Monsivais & Hausser, 2003). With more substantial stimulation, dendritic Ca^{2+} spikes produce an intense depolarization that evokes a burst of Na^+ spikes, thereby coupling dendritic Ca^{2+} spike discharge to somatic Na^+ spike output. Clustering of Purkinje cell Na^+ spikes into bursts of high-frequency discharge provides a powerful inhibitory control over the activity of cerebellar nuclear neurons (Llinas & Sugimori, 1980a,b; Stuart & Hausser, 1994; Telgkamp & Raman, 2002). It was recently reported that climbing fibre EPSP waveforms and dendritic Na^+ spikes can activate Kv3.3/3.4 channels recorded in the outside-out patch configuration from Purkinje cells (Martina *et al*., 2003). However, the ability for Kv3 channels to regulate active Na^+ or Ca^{2+} spike discharge under physiological conditions remains to be determined.

The present study tested the hypothesis that Kv3 channels repolarize somatic and dendritic spike discharge to shape spike and burst output in rat Purkinje cells. We establish that pharmacologically isolated Kv3 currents in outside-out patch recordings are rapidly activating and slowly inactivating. Under current-clamp conditions, Kv3 channels are shown to repolarize both Na^+ and Ca^{2+} spike discharge to regulate spike frequency and burst output. Kv3 channels are further shown to function in tandem with large-conductance Ca^{2+}-activated K^+ channels (BK) to restrain Ca^{2+} spikes to within a range that prevents Na^+ spike inactivation, thereby enabling burst output.

Materials and methods

Animal care

Sprague–Dawley rat dams with litters were obtained from Charles River (Charles River, Canada) and maintained by the Animal Resources Center according to the guidelines of the Canadian Council on Animal Care.

Correspondence: Dr R. W. Turner, as above.
E-mail: rwturner@ucalgary.ca

Received 22 April 2004, revised 2 June 2004, accepted 7 June 2004

doi:10.1111/j.1460-9568.2004.03539.x

Preparation of tissue slices

All drugs were obtained from Sigma, unless otherwise indicated. Artificial cerebrospinal fluid (aCSF) was always composed of (in mM): NaCl, 125; KCl, 3.25; $CaCl_2$, 1.5; $MgCl_2$, 1.5; $NaHCO_3$, 25; D-glucose, 25; preoxygenated by carbogen (95% O_2, 5% CO_2) gas.

Male Sprague–Dawley rats ($n = 80$), age P11–38, were anaesthetized subcutaneously with Pentothal (sodium pentobarbital) and perfused transcardially with 60 mL of ice-cold aCSF at approximately 2 mL/s. The rat was decapitated, the brain exposed and the cerebellum quickly removed and bathed in ice-cold aCSF. The cerebellum was transected in the parasagittal plane by scalpel cut and mounted with cyanoacrylate glue on an ice-cold cutting tray of a Vibratome (Ted Pella, Redding, CA, USA). Parasagittal tissue slices of 300 μm thickness were cut from the cerebellar vermis in ice-cold and carbogen-bubbled aCSF. Each slice was immediately transferred to carbogen-bubbled aCSF maintained in a 35 °C water bath and incubated for 30–45 min; upon removal from the water bath slices were allowed to cool and remain at room temperature (22 °C) before recordings.

Electrophysiology

Slices were transferred to the recording chamber of a Zeiss Axioskop FS-2 microscope maintained at 35 °C. A limited number of recordings were completed at room temperature for comparison. Slices were held in place by a 'harp' consisting of a nylon-strung platinum wire and maintained as a submerged preparation continuously perfused by oxygenated aCSF at a rate of approximately 2 mL/min. Purkinje cells were visualized with differential interference contrast-infrared optics and a Dage MTI Newvicon camera (Michigan City, IN, USA) linked to a video monitor (Hitachi VM9012U; Stuart *et al*., 1993).

Pipettes were pulled from thick-walled (fibre-filled) borosilicate glass (1.5 mm O.D.; A-M Systems, Carlsborg, WA, USA) with a Sutter P-87 puller (Sutter, Novato, CA, USA). The electrolyte for whole-cell current-clamp recordings was adjusted to closely approximate physiological thermodynamic potentials for key ion species at 35 °C: E_{Na} 55.9 mV; E_K −97 mV; E_{Cl} −76 mV. The electrolyte consisted of (in mM): K-gluconate, 130; EGTA, 0.1; HEPES, 10; NaCl, 7; $MgCl_2$, 0.3; pH 7.3 with KOH. Di-tris-creatine phosphate, 5; Tris-ATP, 2; Na-GTP, 0.5 were added daily from frozen stock solutions. A liquid junction potential with the external bathing medium of ∼11.6 mV was calculated for this electrolyte. When absolute membrane voltages are reported in the text they have been corrected for this potential difference. For comparison, several recordings were completed with K-methylsulphonate (130 mM) substituted for K-gluconate. Similar results were obtained with both intracellular solutions. Outside-out recordings identifying the currents affected by tetraethylammonium (TEA) used an electrolyte consisting of (in mM): KCl, 140; EGTA, 0.1; HEPES, 10; NaCl, 7; $MgCl_2$, 0.3; di-tris-creatine phosphate, 5; Tris-ATP, 2; Na-GTP, 0.5; pH 7.3. Patches were immediately rejected if re-sealing to >1 GΩ during patch formation did not occur, or if current levels were unstable during the first 30 s of recording. Patches were rejected *post hoc* if currents following TEA washout did not recover to baseline values, suggesting that rundown of the patch had occurred. Thus, the outside-out patch recordings entered into the analyses were stable for at least 5 min. Whole-cell recording pipettes had a resistance of 4–8 MΩ for somatic and 8–12 MΩ for dendritic recordings, and outside-out pipettes had resistances of 6–8 MΩ. Once formulated, the syringe containing electrolytes was maintained at 4 °C and used for no more than 4 h. In some cases electrodes contained 0.1% neurobiotin for subsequent histological processing.

Whole-cell current-clamp recordings were obtained at 35 °C using an Axoclamp 2A amplifier (Axon Instruments, Foster City, CA, USA) in bridge mode or an Axopatch 200B amplifier in fast current-clamp mode, while outside-out recordings were obtained at room temperature using an Axopatch 200B. Data were collected with pCLAMP 8.1 software (Axon Instruments) operating on IBM-compatible hardware. Whole-cell recordings were filtered at 10 kHz and outside-out recordings at 5 kHz, with any leak subtracted on-line. Purkinje cells were easily identified by their distinct morphology and position within the cerebellar cortex, and selected primarily on the basis of membrane appearance and accessibility of dendrites. The majority of somatic recordings were obtained from P21–38 rats, and dual somatic-dendritic recordings were obtained from P11–19 rats. Purkinje cell dendrites could not be readily visualized in slices from older animals (> P25). However, in all neurobiotin-filled cells from older animals, the presence of an intact dendritic arbor was confirmed by subsequent histological processing and visualization by streptavidin-Cy3 ($n = 15$). Recordings were accepted for use only for initial seal formations of 2 GΩ or greater. An average bias current of −1.4 nA was applied in current-clamp mode to stop spontaneous discharge and maintain all recordings at a baseline level of −70 mV. After whole-cell break-in cells were rejected if the average membrane potential during spontaneous activity was more depolarized than −45 mV.

Pharmacology

Drugs were bath-applied or added to a pressure-ejection electrode containing HEPES-buffered aCSF consisting of (in mM): NaCl, 150; KCl, 3.25; $CaCl_2$, 1.5; $MgCl_2$, 1.5; HEPES, 10; D-glucose, 20; pH 7.4. Current-clamp recordings began 2 min after the onset of drug perfusion (see Fig. 1C and D for time course of TEA effects). Wash-in and washout times for outside-out patch recordings were both approximately 15–20 s. Thus, outside-out recordings were initiated approximately 30 s after perfusion onset. The spatial extent of pressure-ejected drugs was confirmed visually by the dispersal zone of red food colouring included in the electrode (1 : 50 dilution). Ejection of the pressure electrode carrier medium containing the dye alone had no measurable effects. All toxins, apart from apamin, margatoxin and linopirdine (all purchased from Sigma), were obtained from Alomone Labs (Israel) and applied at working concentrations of: α-dendrotoxin (DTX; 200 nM), charybdotoxin (CBTX; 100 nM), iberiotoxin (IBTX; 200 nM), tetrodotoxin (TTX; 100 nM), apamin (200 nM), margatoxin (MGTX; 100 nM) and linopirdine (10 μM). All toxins were prepared daily from frozen stock solutions. Apamin was first dissolved in 50 mM acetic acid and linopirdine in 3% ethanol before preparing stock solutions. Pressure-ejection media supplemented with 3% ethanol alone had no discernable effects. The perfusion media for all toxins was supplemented with 0.1% bovine serum albumin to minimize non-specific binding. All recordings were carried out in synaptic blockers that were bath applied after obtaining the initial seal: picrotoxin (50 μM), D,L-2-amino-5-phosphonopentanoic acid (25 μM), 6,7-dinitroquinoxolinedione (10 μM; Tocris Cookson, Ellisville, MO, USA) and CGP 55845 (1 μM; Tocris Cookson). The same concentration of synaptic blockers was added to the pressure electrode carrier medium for ejections during current-clamp recordings.

Measurements

Data analysis was completed off-line with Clampfit 8.1 (Axon Instruments), and figures prepared in Corel Draw (Ottawa, Canada)

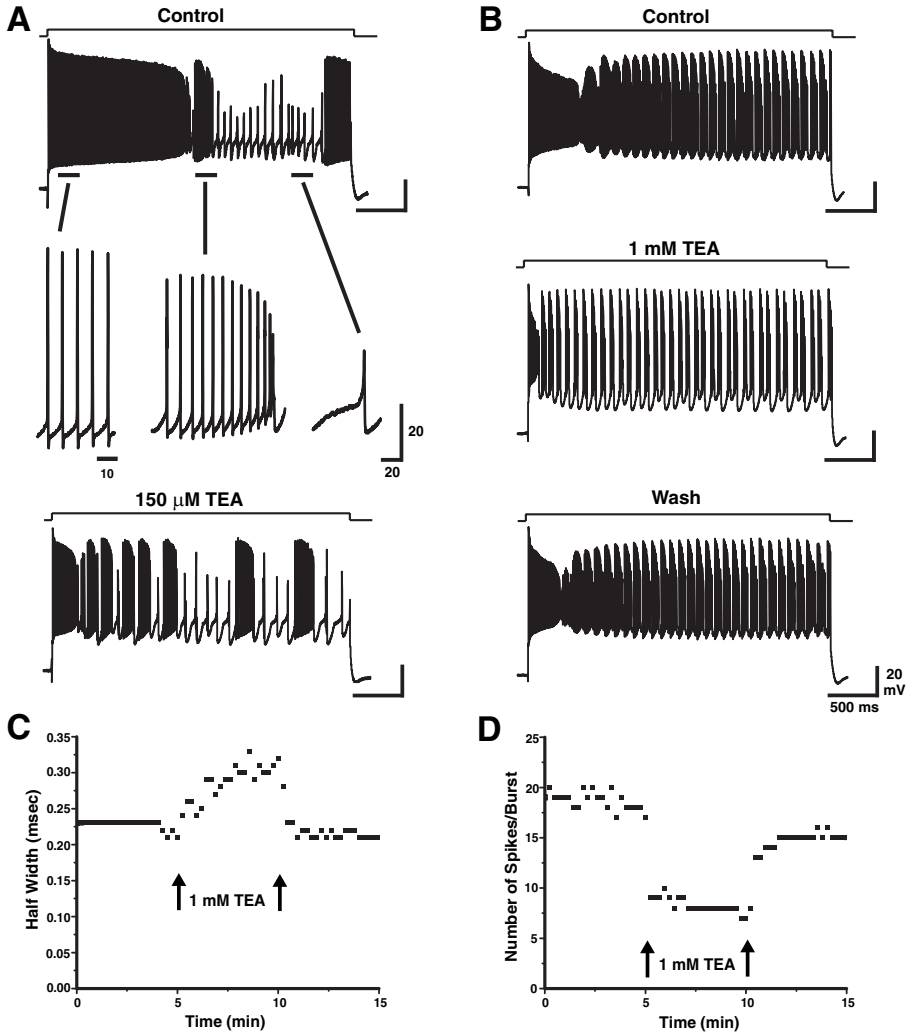

FIG. 1. Low concentrations of tetraethylammonium chloride (TEA) alter Na^+ and Ca^{2+} spike discharge patterns. (A) Three forms of spike discharge recorded at the soma at 35 °C in response to square-wave current-pulse injections (3000 ms). Below are expanded records from within the indicated segments of tonic spike discharge (left), Ca–Na spike bursts (centre) and Ca^{2+} spikes (right). Perfusion of 150 μM TEA induces a progressively greater incidence and magnitude of Ca–Na spike burst discharge. (B) Perfusion of 1 mM TEA induces a prominent shift in the output of the Purkinje cell; all changes are reversible upon washout. The half-width of Na^+ spikes (C) and the number of Na^+ spikes within Ca–Na spike bursts (D) are stationary prior to TEA application. Both parameters are rapidly changed following TEA application (arrows at 5 min) and are stable throughout the 5-min perfusion period. A rapid return to near baseline levels is evident following cessation of TEA perfusion (arrows at 10 min; values in C and D from same cell as in B). Current pulses in (A), 2.4 nA (top) and 2.7 nA (bottom); (B), (C) and (D), 1.2 nA (different cell than in A).

and Adobe Illustrator 9.0 (San Jose, CA, USA). All measurements of spike characteristics were referenced to the initial membrane potential at the point of inflection, signifying the rising edge of the action potential. From this value was calculated the spike height, half-width (duration at half amplitude) and afterhyperpolarization (AHP) amplitudes. The rate of repolarization and total spike durations were calculated using the point at which the falling edge of the action potential reached the reference point membrane potential. Measurements on isolated Ca^{2+} spikes were focused on the final peak depolarization most likely to reflect Ca^{2+} current activation. That this peak depolarization did not include a Na^+ component was confirmed by repeating these experiments in the presence of TTX ($n = 6$). The Ca^{2+} spikes evoked in TTX were also abolished by 2 mM Co^{2+} or 200 μM Cd^{2+}. Alternatively, the advantages provided by dual somatic-dendritic recordings with minimal dendritic Na^+ spike superimposition allowed Ca^{2+} spikes contributing to somatic Ca–Na spike bursts to be unambiguously identified. Given this, data for the two forms of Ca^{2+} spike discharge were pooled in Fig. 6.

For Ca–Na spike bursts, burst duration refers to the time from the onset of the first Na^+ spike evoked by the underlying membrane depolarization to the time on the falling phase of the terminal Ca^{2+} spike corresponding to the same voltage level as the initial Na^+ spike inflection potential. Na^+ spike frequency was measured as the instantaneous frequency of the first two spikes evoked in a tonic discharge or as the average spike frequency during a burst pattern. Statistical analyses were completed with SPSS V10 (SPSS, Chicago, IL, USA). Criterion for statistical significance of the Student's *t*-test was set at $P < 0.05$. Average values represent mean ± SEM. Data are derived from approximately 300 Purkinje cells.

Results

Purkinje cell Na^+ and Ca^{2+} spike discharge patterns

Our recorded patterns of spike activity closely matched previous *in vitro* and *in vivo* recordings conducted near 35 °C (Latham & Paul,

1971; Llinas & Sugimori, 1980b; Pouille *et al*., 2000; Womack & Khodakhah, 2002a, 2003; Edgerton & Reinhart, 2003). The average somatic input resistance as determined by hyperpolarizing steps was 30.3 ± 1.9 MΩ ($n = 62$). Purkinje cells typically discharged Na^+ spikes at a spontaneous rate of 7–153 Hz (67.4 ± 6.6 Hz, $n = 30$) that were often followed by a spontaneous discharge of Ca^{2+} and Na^+ spike bursts (referred to here as Ca–Na spike bursts) and then periods of silence, similar to the trimodal pattern of discharge of Womack & Khodakhah (2002a, 2003, 2004). When present, a trimodal pattern was considered representative of healthy neurons as it could be recorded early or late in a recording session and persisted unaltered in form for hours. It was not, however, readily observed at 22 °C, perhaps accounting for the lack of reports of this pattern in other *in vitro* studies. Consistent with this, we found that the incidence of spontaneous Ca^{2+} spikes and Ca–Na spike bursts was higher, and the threshold for evoking these responses much lower for recordings at 35 °C compared with 20 °C (Womack & Khodakhah, 2002a).

We found that TEA applied at even 50 μM decreased input resistance by 20 ± 5.5% ($n = 11$). This result may reflect an increase in spontaneous transmitter release subsequent to block of Kv3 channels distributed on synaptic terminals in the Purkinje cell body layer and molecular layer (Southan & Robertson, 2000; Matsukawa *et al*., 2003). All recordings were thus carried out in the presence of blockers of ionotropic glutamate receptors (APV and 6,7-dinitroquinoxolinedione) and γ-aminobutyric $acid_A$ (picrotoxin) and γ-aminobutyric $acid_B$ (CGP 55845) receptors. No significant change in input resistance was apparent upon application of these blockers, or after perfusion of 150 μM ($n = 11$) or 1 mM TEA ($n = 25$) in the presence of synaptic blockers.

The present study focused on spike discharge patterns evoked by square-wave current-pulse injections up to 4.2 nA and 3000 ms duration. Current injection in the range of 1–2 nA from a holding potential of −70 mV evoked a tonic series of fast Na^+ spikes that could inactivate over time (Fig. 1A). Na^+ spike inactivation coincided with the rise of an underlying membrane depolarization that led to a final Ca^{2+} spike. Termination of Na^+ spike discharge was followed by two forms of Ca^{2+} spike discharge at a relatively fixed rate of 23 ± 2 Hz (1.8 nA; $n = 16$). At low levels of current injection, large amplitude Ca–Na spike bursts predominated, while later in a current pulse, and more often at higher levels of current injection, Ca^{2+} spikes without accompanying Na^+ spikes were generated (Fig. 1A). This pattern of Ca^{2+} spike activity was not fixed, in that Ca–Na spike bursts and Ca^{2+} spikes could occur interchangeably.

TEA shifts the pattern of Na^+ and Ca^{2+} spike discharge

Cerebellar Purkinje cells have been shown to express both Kv3.3 and Kv3.4 K^+ channel subunits (Goldman-Wohl *et al*., 1994; Weiser *et al*., 1994; Rashid *et al*., 2001a; Martina *et al*., 2003). Unlike many Kv channel subtypes, few toxins exist to block Kv3 channels, although all of the Kv3 channel subtypes exhibit a high sensitivity to TEA and 4-aminopyridine (4-AP; micromolar range; Coetzee *et al*., 1999). Outward currents activated in outside-out patch recordings or dissociated Purkinje cell somata have an IC_{50} for TEA of ∼150 μM and for 4-AP of ∼270 μM (Southan & Robertson, 2000; Bushell *et al*., 2002; Martina *et al*., 2003). In isolated mouse Purkinje cells, 1 mM TEA blocks all spike-associated outward current (Raman & Bean, 1999) and reduces outward currents in outside-out patches extracted from rat Purkinje cells by up to 79% (Martina *et al*., 2003). Application of TEA at low concentrations can thus be predicted to have marked effects on Purkinje cell Kv3 K^+ currents. We did not apply 4-AP given that the IC_{50} for 4-AP is within the range to affect all Kv1.x, Kv2.x and Kv3.x channels (Coetzee *et al*., 1999), and did not use BDS toxins to block Kv3.4 channels given the voltage-dependent actions of these compounds (Baranauskas *et al*., 2003). We thus sought to determine the role for Kv3 currents in regulating Purkinje cell Na^+ and Ca^{2+} spike discharge using TEA as a blocking agent, without specific reference to the Kv3 channel subtype.

As an initial test of the potential for Kv3 currents to affect spike output, we bath-perfused or pressure-ejected either 150 μM or 1 mM TEA (Fig. 1A and B). TEA at 150 μM consistently shifted the pattern of spike output towards the generation of more Ca–Na spike bursts and Ca^{2+} spikes (Fig. 1A; $n = 11$). These effects were substantially increased in 1 mM TEA, but were extended to include more intense Ca–Na spike bursts, with fewer Na^+ spikes per burst (Fig. 1B; $n = 25$). A similar shift towards the generation of large-amplitude AHPs following Ca^{2+}-dependent spikes was observed with increasing concentrations of TEA (Fig. 1B). Cell output, as demonstrated by half-width of Na^+ spikes and the number of Na^+ spikes per Ca–Na burst, was stable for long periods prior to and during drug application (Fig. 1C and D). In the absence of any manipulation, cell output was stationary over very long periods (> 30 min). With our local perfusion system drug wash-in occurred in less than 1 min, and washed-out just as rapidly (Fig. 1C and D). All output parameters could be recovered to near baseline levels following washout of TEA (Fig. 1B–D). Similar stationary results were observed before and during CBTX application, the other principal toxin used in this study, although this toxin did not washout.

Multiple TEA-sensitive K^+ currents are activated under physiological conditions

Although the above tests are expected to block Kv3 K^+ channel subunits, the IC_{50} for other K^+ channels expressed in Purkinje cells falls near that of Kv3 channels. These include *Shaker* subtypes Kv1.1 ($IC_{50} = 500$ μM) and Kv1.6 ($IC_{50} = 1.7$–7.0 mM), Ca^{2+}-activated BK channels (slo1 $IC_{50} = 80$–330 μM) and KCNQ2 channels ($K_d = 160$ μM) (Wang *et al*., 1998a; Coetzee *et al*., 1999). The protein or transcripts for each of these channels have been localized to Purkinje cells (Veh *et al*., 1995; Knaus *et al*., 1996; Chung *et al*., 2001; Saganich *et al*., 2001) and could thus be potentially blocked by micromolar concentrations of TEA.

We were particularly interested in any block by TEA of these channels under the recording conditions present in the whole-cell current-clamp configuration. To examine this, outside-out macropatch recordings were obtained from somatic membrane using an electrolyte that closely resembled that used for whole-cell current-clamp recordings (see Materials and methods). These experiments were designed to activate the full suite of currents potentially sensitive to TEA over the voltage range traversed by Na^+ and Ca^{2+} spikes. TTX was included in the bathing medium to block Na^+ currents.

Step commands from −70 mV to 30 mV revealed a net outward current of 808 ± 41 pA ($n = 109$) that was fast activating and slowly inactivating (Fig. 2A). The degree of inactivation over 200 ms was variable, although all recordings showed evidence of an initial early peak with a moderate amount of inactivation by the end of the step command (28.0 ± 1.6%; $n = 109$). TEA produced a concentration-dependent block, with perfusion of 150 μM TEA blocking 21.5 ± 3.8% ($n = 9$) of the current and 1 mM TEA blocking 61.5 ± 4.0% ($n = 15$) (Fig. 2A and C). The relative amount and nature of the current remaining after 1 mM TEA was variable, although a small amount of outward inactivating current could be seen in some cases.

Purkinje cells express mRNA for KCNQ2 channels (Saganich *et al*., 2001), and the KCNQ inhibitor linopirdine depresses ∼10% of

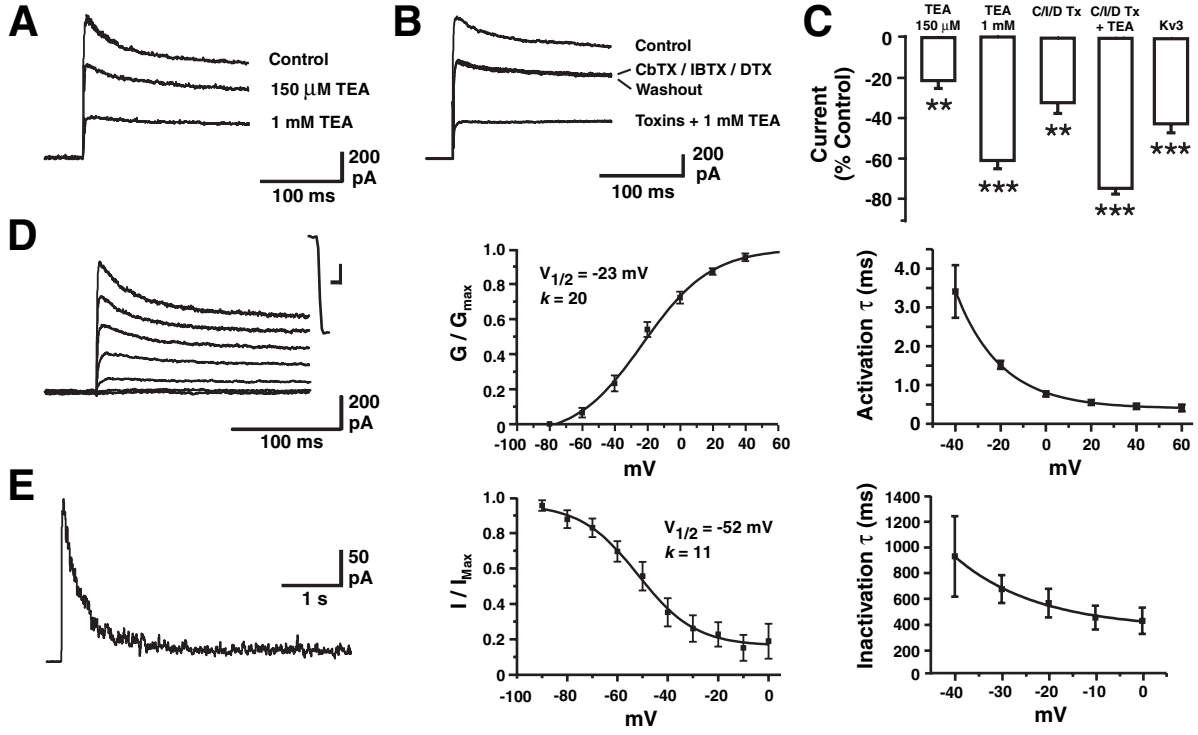

FIG. 2. Purkinje cells express multiple tetraethylammonium chloride (TEA)-sensitive K^+ currents. (A and B) Representative outside-out macropatch recordings obtained from Purkinje cell somata under conditions resembling those used for whole-cell current-clamp recordings. All records are averages of 5–15 sweeps for currents evoked by a 200-ms step command from −70 to 30 mV in 0.1 μM tetrodotoxin (TTX). (A) The step command reveals a fast activating and slowly inactivating ensemble outward current that is rapidly blocked by local perfusion of 150 μM or 1 mM TEA. (B) Combined perfusion of charybdotoxin (CBTX), iberiotoxin (IBTX) and α-dendrotoxin (DTX) reduces the outward current, with additional block by subsequent addition of the combination of these toxins and 1 mM TEA. Although the effects of TEA are rapidly reversible, the effects of toxins are not (toxin recordings and those obtained after washing TEA and toxins are shown superimposed). (C) Plots of the average percentage change of current evoked at 30 mV after 150 μM TEA, 1 mM TEA, combined CBTX/IBTX/DTX (C/I/DTX), C/I/DTX and 1 mM TEA, or after subtracting C/I/DTX-sensitive current from TEA-sensitive current (isolating putative Kv3.x currents). Values are normalized to control (0%). (D) Current–, conductance– and activation tau–voltage relationships of Kv3.x current isolated by subtracting currents recorded in 1 mM TEA from control records obtained in the presence of CBTX/IBTX/DTX. The activation plot was constructed from a holding potential of −80 mV with consecutive 20-mV steps to 60 mV for 200 ms ($n = 7$). Inset in subtracted traces is the deactivation current elicited by a repolarization from 60 mV to −80 mV; calibration bars for inset are 200 pA and 0.5 ms. (E) Slowly inactivating Kv3 currents were revealed by subtracting currents obtained in 1 mM TEA from control records obtained in the presence of CBTX/IBTX/DTX during 5-s step commands from −90 mV to 0 mV in 10-mV increments. Conductance and inactivation plots were fit with a Boltzmann function ($y = 1/(1 + \exp[(V - V_{½})/k]$) using an E_K of −95 mV. Activation taus were fit with a power relationship and inactivation taus with a single exponential function. Asterisks in (C) indicate significance of test vs. control recordings: $^{**}P < 0.01$; $^{***}P < 0.001$; Student's *t*-test.

non-inactivating outward currents in mouse Purkinje cells (Bushell *et al.*, 2002). Outside-out patches were stepped from −70 mV to 20 mV for 2 s and then back to −50 mV for 6 s to detect the slow deactivation that characterizes M-like currents (Brown & Adams, 1980; Wang *et al.*, 1998a). We could detect no slowly deactivating KCNQ-like current in our cells ($n = 9$), and there was no effect by linopirdine (10 μM) on the current evoked on return to −50 mV ($n = 3$; data not shown). Linopirdine did reduce outward currents evoked during the step command from −70 to 30 mV by 48.2 ± 1.6% ($n = 7$). However, we found that 10 μM linopirdine also blocked 52.2 ± 2.6% of the peak mammalian Kv3.3b currents expressed in isolation in Chinese Hamster Ovary cells and a similar percentage of the steady-state current ($n = 6$; data not shown), indicating that linopirdine cannot be used to distinguish between Kv3 and KCNQ2 currents. By comparison, CBTX, the other principal toxin used in this study, had no measurable effects on expressed Kv3.3b currents ($n = 4$). Given the lack of evidence for KCNQ2-like currents over the voltage range examined here, we concluded that TEA effects on rat Purkinje cells are not mediated by KCNQ2 channels.

IBTX has been reported to have little effect on Purkinje cell activity under current-clamp recording conditions unless presented in combination with other ion channel blockers (Edgerton & Reinhart, 2003; Womack & Khodakhah, 2004). We therefore applied both IBTX and CBTX to block BK channels. The potential activation of TEA-sensitive *Shaker*-class K^+ channels was tested by co-perfusing 200 nM DTX. A cocktail of CBTX/IBTX/DTX blocked 32.3 ± 5.2% of current evoked by a step command from −70 mV to 30 mV ($n = 12$; Fig. 2B and C). We further determined in separate experiments that 9.3 ± 2.4% of this block could be attributed to DTX-sensitive currents ($n = 10$). Subsequent application of TEA (1 mM) in the presence of the toxin cocktail decreased the current by a total of 74.6 ± 2.7% with respect to control ($n = 12$; Fig. 2B and C). Whereas TEA could be completely washed-out within seconds following termination of TEA application, the effects of the toxin cocktail were irreversible. Therefore, after consideration of non-Kv3 TEA-sensitive currents, the putative Kv3 channel component accounted for 42.4 ± 4.4% of the total current in outside-out patches (Fig. 2C).

Subtraction of CBTX/IBTX/DTX-sensitive currents from the total TEA-sensitive response isolated the current presumably mediated by Kv3 channels (Fig. 2C–E; $n = 12$). The isolated (TEA-subtracted) Kv3 current was 376.6 ± 46.5 pA ($n = 12$) at peak amplitude when activated by a step from −70 mV to 30 mV, with 26.5 ± 3.2%

inactivation over a 200-ms pulse command (Fig. 2D). A Boltzmann function fit of the conductance plot indicated a $V_{1/2}$ for activation of −23.0 mV and a slope factor $k = 20.6$ (Fig. 2D). Deactivation of the isolated Kv3 current was extremely rapid, with a time constant of 0.66 ms (SD = 0.29) for a step from 60 mV back to −80 mV ($n = 3$). Long step commands (5 s) from a holding potential of −90 mV revealed a slow inactivation of the isolated Kv3 current with $V_{1/2}$ of −51.7 mV and $k = 11.4$ (Fig. 2E). The tau for both activation and inactivation proved to be voltage-dependent over the range of −40–0 mV (Fig. 2D and E). We note that the half activation for Kv3 currents in Purkinje cells overlaps ideally with the voltages traversed by both Na^+ spikes (mean takeoff to peak voltage: −55 to 8 mV) and Ca^{2+} spikes (mean takeoff to peak voltage: soma, −35 mV to 24 mV; dendrites, −40 mV to 8 mV), thus positioning these channels to participate in the repolarization of both responses.

Identifying Kv3-like currents contributing to spike output

These studies establish the potential for low concentrations of TEA to affect three K^+ channel classes in Purkinje cells: Kv3.x, DTX-sensitive Kv1.x and IBTX/CBTX-sensitive BK channels. For this reason, current-clamp recordings using TEA to identify the physiological role of Kv3 channels also included tests on the effects of IBTX, CBTX and DTX. DTX-sensitive currents contributed to several important aspects of Purkinje cell output, although the effects were very different from TEA application. Because CBTX can also block some Kv1 channels, particularly Kv1.3 (Coetzee *et al*., 1999), we compared the Kv1.3 blocker MGTX (100 nM) to CBTX. MGTX resulted in identical effects to DTX, which were both very different from CBTX. Thus, we can rule out the effects of CBTX on Kv1 channels for the spike properties reported here. We found that IBTX did not have any significant effects on the spike parameters measured here, while CBTX did affect some of the parameters affected by TEA (see Discussion). We therefore restrict our description to results obtained with TEA and CBTX unless otherwise indicated. However, as reported below, in many cases the effects of TEA were distinct or greater than those produced by CBTX, allowing us to distinguish several putative Kv3-mediated responses.

Kv3 K^+ channels repolarize Purkinje cell Na^+ and Ca^{2+} spikes

Na^+ spikes

Perfusion of 150 μM TEA slowed the rate of repolarization of Na^+ spikes by approximately 25% and attenuated the fast AHP (Fig. 3A and B; $n = 11$). TEA at 1 mM slowed the rate of repolarization by over 50% and abolished the fast AHP (Fig. 3A and B; $n = 16$), while CBTX significantly increased the rate of repolarization but did not affect the fast AHP (Fig. 3A and B; $n = 11$). The change in rate of spike repolarization and half-width with TEA was apparent over the full range of current intensities, with even greater changes at higher intensities (data not shown). A decrease in the rate of spike repolarization with TEA would be expected to decrease spike frequency (Erisir *et al*., 1999). Under control conditions, Purkinje cells fired trains of Na^+ spikes at 150 to over 400 Hz in response to 1.5–3.9 nA current injections. TEA reduced the ability for spikes to discharge repetitively, but only decreased spike frequency during burst discharge (Fig. 3B). Previous work suggests that Ca^{2+}-activated K^+ channels play a key role in establishing Na^+ spike frequency (Edgerton & Reinhart, 2003; Womack & Khodakhah, 2004). Consistent with this, we found that blocking BK channels with CBTX significantly increased spike frequency (Fig. 3B; $n = 11$). We thus attribute the absence of a net change in tonic Na^+ spike frequency following TEA perfusion to the simultaneous block of BK and Kv3 channels. As BK channels played a less significant role in determining Na^+ spike frequency within bursts (see Fig. 3B), a reduction in intraburst discharge frequency with TEA was more evident. Collectively these results suggest that Kv3 channels are critical for the control of Na^+ spike repolarization, the generation of fast AHPs and for high-frequency discharge in Purkinje cells. Calcium-activated K^+ conductances provide an additional control over Na^+ spike frequency.

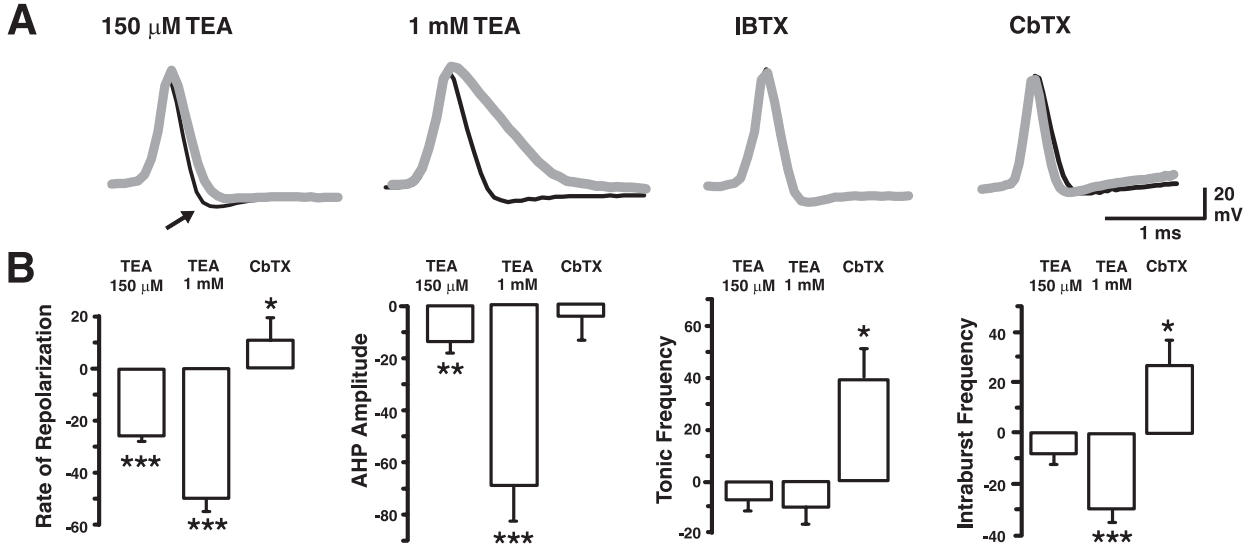

FIG. 3. Kv3 K^+ channels repolarize Na^+ spikes and generate a fast AHP. (A) Superimposed representative somatic recordings before (black trace) and after (grey trace) bath perfusion of 150 μM or 1 mM tetraethylammonium chloride (TEA), iberiotoxin (IBTX) or charybdotoxin (CBTX). TEA at 150 μM slows spike repolarization and reduces the fast AHP (arrow), while 1 mM TEA dramatically slows spike repolarization. IBTX had no affect on spike discharge, suggesting that BK currents are IBTX-insensitive but CBTX-sensitive. Note that the net effects of TEA are distinct from any produced by CBTX alone. (B) Plots of the percentage change of various parameters of Na^+ spike discharge after application of TEA or toxins, normalized to control values (0% change) for 1.8 nA current injection. Asterisks indicate significance of test vs. control recordings: $*P < 0.05$; $**P < 0.01$; $***P < 0.001$; Student's *t*-test.

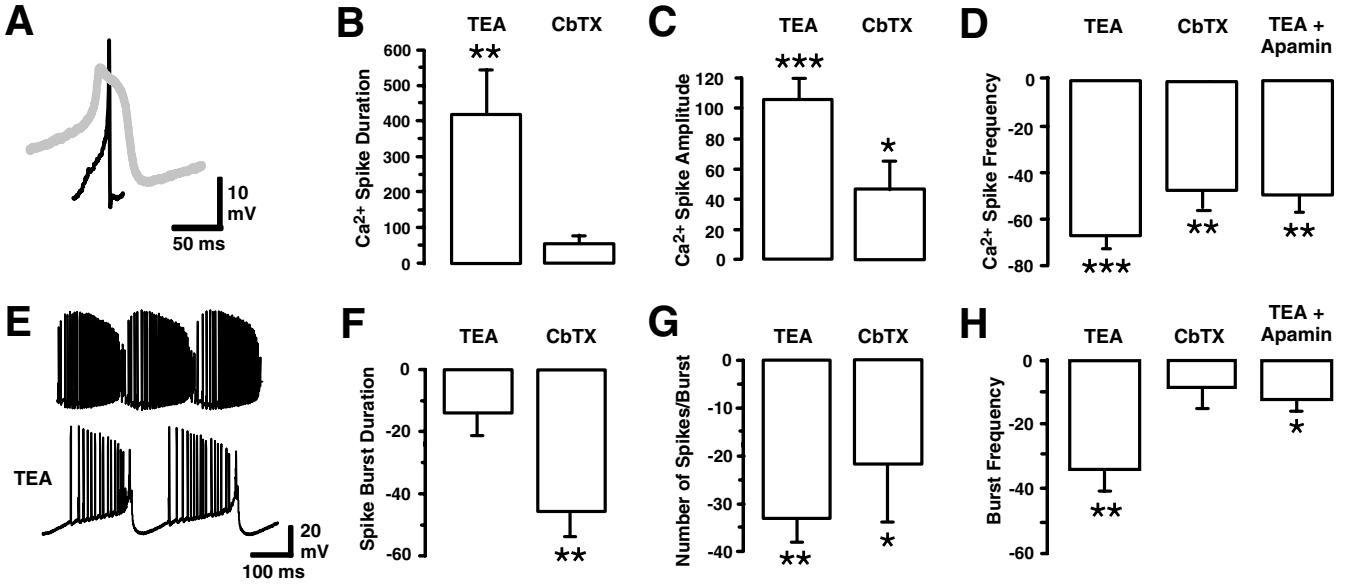

FIG. 4. Kv3 K^+ channels repolarize Ca^{2+} spikes. (A) Superimposed somatic recordings of isolated Ca^{2+} spikes before (black trace) and after (grey trace) 1 mM tetraethylammonium chloride (TEA). (B–D) Plots of the percentage change of various parameters related to Ca^{2+} spike discharge after application of 1 mM TEA or CBTX. Values are normalized to control (0%) for 3.0 nA current injection. TEA increases the duration (B) and amplitude (C) of Ca^{2+} spikes, and lowers Ca^{2+} spike frequency (D), revealing a role for Kv3 channels in repolarizing Ca^{2+} spikes. (E) Somatic recordings of Ca–Na spike bursts before and after 1 mM TEA. (F–H) Plots of the percent change of spike and burst parameters in 1 mM TEA or charybdotoxin (CBTX) normalized to control values (0%). A competing effect between Kv3 and BK channels on spike burst duration was revealed by a mismatch between TEA and CBTX effects (F; compare with B). The number of Na^+ spikes per burst was controlled primarily by BK K^+ channels (G), whereas burst frequency was controlled more by TEA-sensitive Kv3 channels (H). The marked slowing of burst frequency following TEA application was attenuated by co-perfusion of 200 nM apamin, indicating a secondary recruitment of SK K^+ channels (H). Asterisks indicate significance of test vs. control recordings: $*P < 0.05$; $**P < 0.01$; $***P < 0.001$; Student's *t*-test.

Ca^{2+} spikes

Larger current injections evoke repetitive discharge of isolated Ca^{2+} spikes and/or Ca–Na spike bursts (Fig. 1). To identify the role for Kv3 channels in regulating Ca^{2+}-dependent responses, we chose to first assess the isolated Ca^{2+} spike. The primary effect of 150 μM TEA was to block a fast AHP component that follows Ca^{2+} spike discharge ($n = 8$). As the changes induced by 1 mM TEA were substantially greater, the average values plotted in Fig. 4A–D were restricted to results obtained with 1 mM TEA ($n = 25$). Perfusion of 1 mM TEA greatly increased the duration and amplitude of Ca^{2+} spikes with a less pronounced effect by CBTX-sensitive conductances (Fig. 4A–C; $n = 10$). A decrease in Ca^{2+} spike frequency by both TEA and CBTX (Fig. 4D) was produced in part by an increase in the subsequent AHP. This increase in the AHP was unrelated to a secondary activation of small conductance (SK) K^+ channels, as co-perfusion of apamin (200 nM) did not prevent the effects by TEA on Ca^{2+} spike frequency (Fig. 4D). These results indicate that Kv3 K^+ channels act to restrain both the amplitude and duration of Ca^{2+} spikes, demonstrating a key role for Kv3 K^+ channels in repolarizing Ca^{2+} spikes. The net result is to maintain a higher frequency of Ca^{2+} spike discharge.

Ca–Na spike bursts

The two most salient modifications in burst output related to a block of Kv3 K^+ channels by TEA was a change in burst duration and a slowing of burst frequency (Fig. 4E–H). Blockade of Kv3 currents could ostensibly increase burst duration by broadening the underlying Ca^{2+} depolarization in the same manner as found for isolated Ca^{2+} spikes (cf. Fig. 4B and F). However, an analysis of burst duration revealed a mismatch between the effects of TEA and CBTX, in that TEA had no significant effect while CBTX substantially shortened burst duration (Fig. 4F), as recently reported for IBTX application (Womack & Khodakhah, 2004). A null result with TEA application might then arise through opposing actions of blocking Kv3 channels (increased Ca^{2+} spike duration) and BK channels (decreased burst duration). An equivalent decrease in the number of spikes generated within each burst by TEA or CBTX suggests a prominent role for BK channels in setting this parameter (Fig. 4G). Blockade of Kv3 channels also slowed burst frequency (Fig. 4H), a result that was mostly prevented by co-perfusing 200 nM apamin ($n = 14$, Fig. 4H). These results emphasize that Kv3 channels restrain the Ca^{2+} depolarization underlying the burst, preventing prolonged Ca^{2+} influxes that trigger the secondary activation of SK K^+ channels that slows burst frequency.

Ca–Na spike coupling

The information transferred from a pre- to postsynaptic cell depends on the pattern and number of Na^+ spikes generated at the axon hillock in response to the summation of dendritic and somatic activity. Purkinje cells exhibit a prominent coupling between dendritic and somatic activity in that large dendritic Ca^{2+} spikes trigger a burst of Na^+ spikes at the soma. Two burst parameters that are expected to influence the nature of postsynaptic potentials evoked in deep nuclear neurons are the frequency of Ca–Na spike bursts and the number of Na^+ spikes triggered by each burst. To further examine this relationship, we carried out dual somatic and dendritic recordings up to 130 μm from the soma to record the effects of 1 mM TEA on burst parameters (Fig. 5; $n = 16$). At low intensities of stimulation the principal output of Purkinje cells was the tonic discharge of Na^+ spikes without underlying Ca^{2+} spikes, a pattern reflected in dendrites as a series of small-amplitude depolarizations (Fig. 5A). After 1 mM TEA,

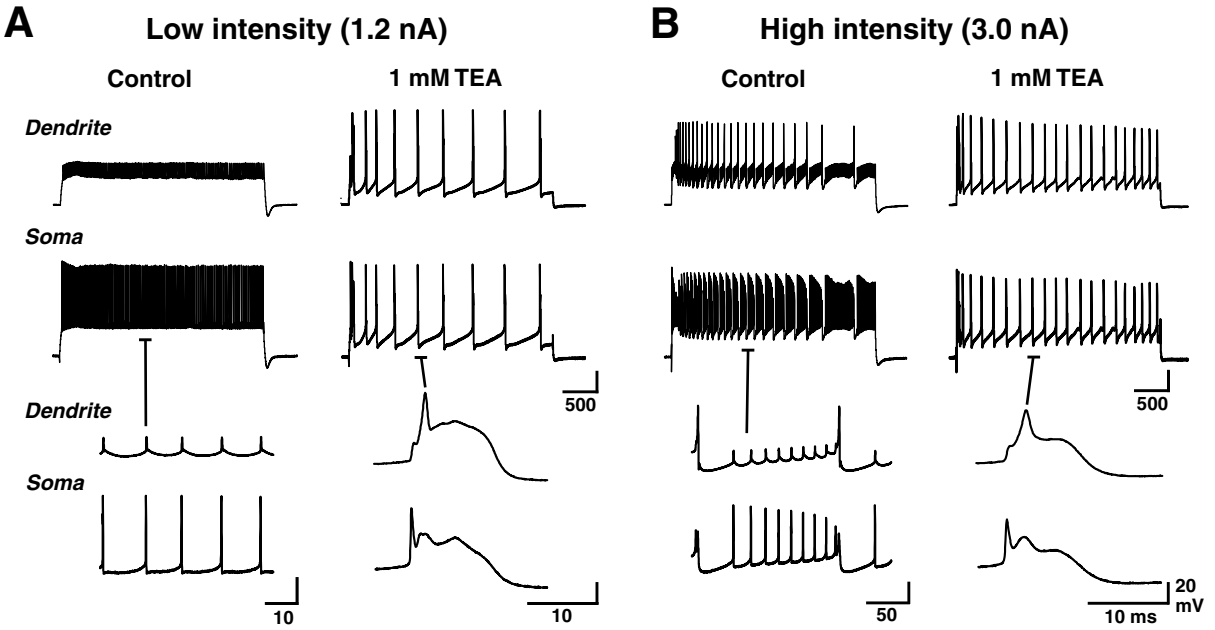

FIG. 5. Blocking tetraethylammonium chloride (TEA)-sensitive K^+ channels results in Na^+ spike inactivation during Ca^{2+} spike discharge. Dual somatic and dendritic (80 μm) recordings of a Purkinje cell in response to (A) low- and (B) high-intensity stimulation using square-wave current-pulse injections (3000 ms). Shown are responses evoked before and after 1 mM TEA, with the bottom two rows illustrating expanded segments of the records above at the positions indicated. TEA converts either tonic Na^+ spike discharge (A, Control) or Ca–Na spike bursts (B, Control) to large amplitude and long-duration Ca^{2+} spikes that rapidly inactivate somatic Na^+ spikes (A and B, TEA).

large-amplitude Ca^{2+} spikes were generated at a lower frequency in both soma and dendrites (Fig. 5A). Closer inspection revealed that in approximately half of the cells the TEA-induced increase in Ca^{2+} spike was so dramatic that Na^+ spikes were almost entirely inactivated (Fig. 5A). Higher stimulus intensities initially evoked a series of Ca–Na spike bursts, with the dendritic component comprised of a large Ca^{2+} spike and small depolarizations reflecting somatic Na^+ spike discharge (Fig. 5B). TEA application at the higher stimulus intensity again shifted spike generation to that of a low-frequency series of Ca^{2+} spikes at both the somatic and dendritic level that substantially inactivated Na^+ spike discharge (Fig. 5B). TEA thus resulted in a net reduction in the number of Na^+ spikes discharged.

To better understand the relationship between Ca^{2+} and Na^+ spike discharge, we examined the effects of TEA over a range of current intensities. The amplitude of the Ca^{2+} spike recorded in the dendrite was consistently larger for all but the lowest levels of current injection ($\sim$ 190% of soma at 2.4 nA), and for all distances from the soma (Fig. 6A and B). As current intensity was increased, the dendritic Ca^{2+} spike amplitude was essentially maintained while the somatic Ca^{2+} spike response decreased by $\sim$45% (Fig. 6A and B). Perfusion of 1 mM TEA increased the amplitude of somatic Ca^{2+} spikes by $\sim$130% and dendritic Ca^{2+} spikes by $\sim$80% ($n = 16$), a relative difference that was maintained over all levels of current injection (Fig. 6A). By comparison, TEA invoked a new response by revealing an intensity-dependent increase in the duration of Ca^{2+} spikes in both soma and dendrite (Fig. 6C; cf. Fig. 4B). Thus, as current intensity increased, Ca^{2+} spike duration increased at the soma from 60% above control values for 0.6 nA current injection to almost 450% above control at 4.2 nA injection (Fig. 6C), representing a 7.5-fold increase across the full intensity range. There was a further intensity-dependent increase in the average duration of the spike burst prior to the Ca^{2+} spike itself (Fig. 6D, 300% increase at 3.6 nA; cf. Fig. 4F), and an intensity-independent decrease in burst frequency (cf. Figs 6E and 4H).

From our earlier results we can assign the TEA-induced changes in Ca^{2+} spike amplitude and duration, changes in the duration of the spike burst and the control of burst frequency shown in Fig. 6A–E to Kv3-mediated processes at both the somatic and dendritic level (Fig. 7). An additional TEA-sensitive BK K^+ channel contribution is evident in a decrease in the number of Na^+ spikes triggered per burst (Fig. 6F). Therefore, Kv3 and BK channels function in concert to repolarize Ca^{2+} spikes (Kv3) and to maintain a high frequency and high number of spikes per burst (Kv3 and BK). Note that the summary diagram of Fig. 7 does not include the role of SK K^+ channels, whose activation is balanced by the repolarizing actions of TEA-sensitive currents, and which play an important role in regulating spike discharge (Cingolani *et al*., 2002; Edgerton & Reinhart, 2003; Womack & Khodakhah, 2003, 2004). Collectively these mechanisms ensure efficient burst output from the Purkinje cell.

Discussion

The current study used low concentrations of TEA in conjunction with other ion channel blockers to identify the contribution of Kv3 K^+ channels to spike discharge and output patterns under physiological conditions. We have established that Kv3 K^+ channels repolarize Purkinje cell Na^+ and Ca^{2+} spike discharge at both the somatic and dendritic level, and perform the important function of limiting Ca^{2+} spike depolarizations to within a range that enables the generation of a burst of Na^+ spikes.

TEA-sensitive currents in Purkinje cells

Previous studies have addressed the effects of 4-AP or TEA application on spike output in Purkinje cells (Llinas & Sugimori, 1980b; Midtgaard *et al*., 1993; Etzion & Grossman, 1998; Seo *et al*., 1999; Sacco & Tempia, 2002; Cavelier *et al*., 2003). For instance,

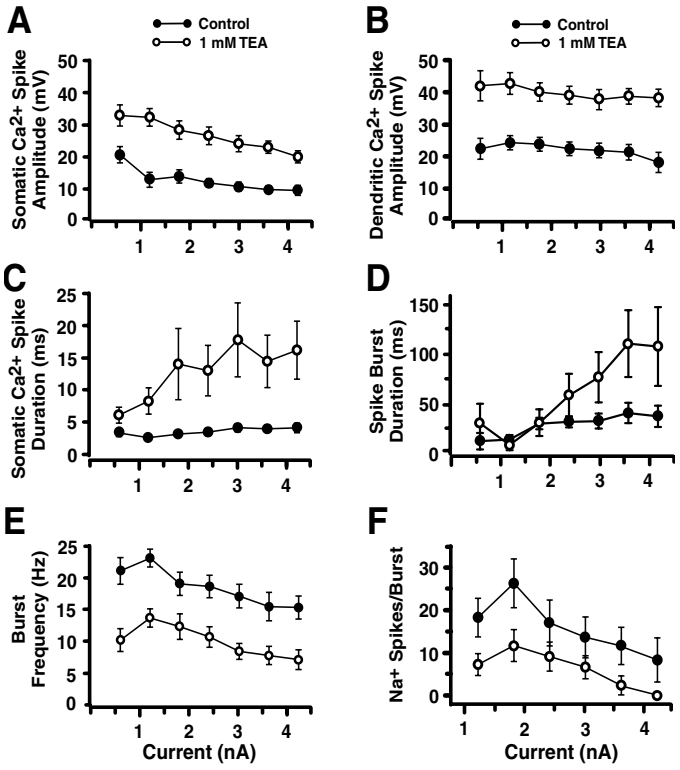

FIG. 6. Tetraethylammonium chloride (TEA)-sensitive K^+ channels maintain an efficient coupling between Ca^{2+} and Na^+ spike discharge. (A–F) Plots of the average absolute values of Ca^{2+} spike and burst discharge parameters under control (filled circles) and in 1 mM TEA (open circles) over a range of square-wave current-pulse intensities (3000 ms; $n = 4$–16 per average). The amplitude of Ca^{2+} spikes recorded with dual somatic (A) and dendritic (B) recordings (20–130 μm). TEA induces an intensity-dependent increase in the duration of somatic Ca^{2+} spikes (C) and the duration of spike bursts (D). TEA invokes a decrease in the frequency of Ca^{2+} spike generation (E) and a concomitant decrease in the number of Na^+ spikes triggered per burst (F).

application of 1 μM–2 mM 4-AP or 2–5 mM TEA has been shown to affect Ca^{2+} spikes and the oscillatory frequency of Purkinje cells (Midtgaard *et al*., 1993; Etzion & Grossman, 1998; Seo *et al*., 1999). However, it is now apparent that 4-AP and TEA block multiple K^+ channels even at micromolar concentrations (Coetzee *et al*., 1999). We did not assess the sensitivity of Purkinje cells to 4-AP, as this drug works only after permeating the cell membrane and accumulating in the cytosol to unknown concentrations.

Purkinje cells are known to express Kv3.3 and 3.4 subunits (Goldman-Wohl *et al*., 1994; Weiser *et al*., 1994; Rashid *et al*., 2001a; Martina *et al*., 2003). A recent voltage-clamp study reported the properties of a TEA-sensitive slowly inactivating current in outside-out recordings under conditions expected to minimize the contribution of Ca^{2+}-activated K^+ channels (Martina *et al*., 2003). We used solutions that approximate physiological conditions and then isolated the Kv3 current contribution by applying blockers for all other potential TEA-sensitive currents. Under these conditions we identified IBTX/CBTX- and DTX-sensitive currents that together blocked ~32% of the net current activated over the voltage range relevant to Na^+ and Ca^{2+} spikes. After removing IBTX/CBTX- and DTX-sensitive currents, we isolated the TEA-sensitive and presumed Kv3.3/3.4 contribution as a fast activating and slowly inactivating current.

The isolated Kv3 current had a $V_{1/2}$ for activation of −23 mV and $V_{1/2}$ for inactivation of −52 mV. These values are left-shifted with respect to reports of most Kv3.x channel subunits when examined in heterologous expression systems (Rudy *et al*., 1991, 1999; Vega-Saenz de Miera *et al*., 1992; Rudy & McBain, 2001; Fernandez *et al*., 2003), and to those previously reported for Purkinje cells (Martina *et al*., 2003). Notably, we obtained very similar values for activation to that of Martina *et al*. (2003) when using the same electrolytes (data not shown). Our values for activation are fairly similar to those reported by Baranauskas *et al*. (2003) when Kv3.1 and 3.4 K^+ channels were co-expressed in HEK293 cells. These authors attributed a leftward shift in the activation voltage for Kv3 currents in fast-spiking neurons to the heteromeric combination of Kv3.1 and Kv3.4a subunits, the latter of which induces a leftward shift in activation. Reports to date suggest that Purkinje cells express one or both of Kv3.4a or 3.4b

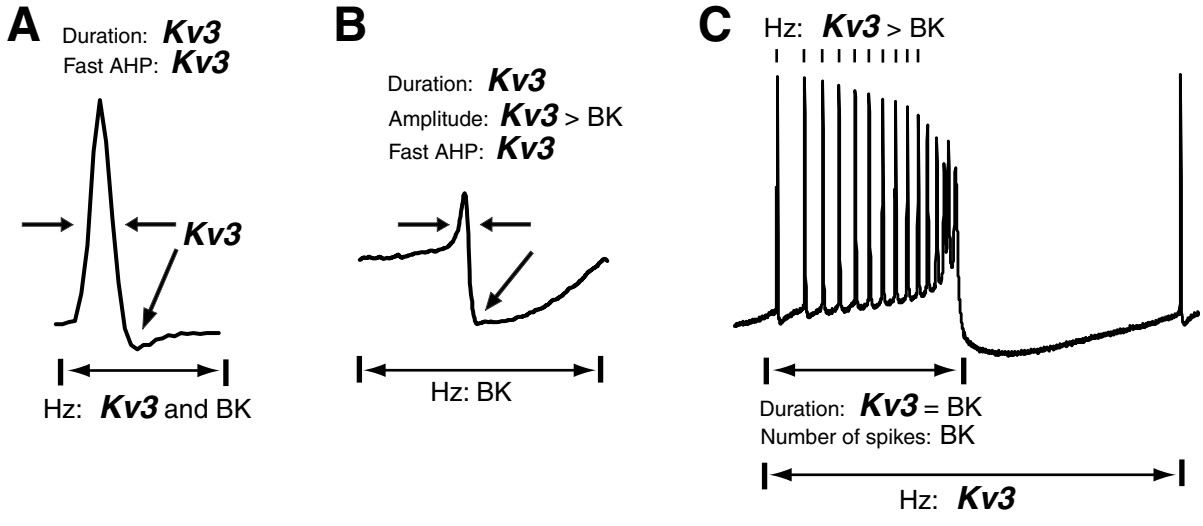

FIG. 7. Schematic summary of the role for Kv3 K^+ currents in Na^+ and Ca^{2+} spike discharge in Purkinje cells. Kv3 K^+ channel contributions are highlighted in *bold* and *italics*. (A) Kv3 K^+ channels mediate the repolarization and fast AHP of Na^+ spikes and contribute to setting tonic spike frequency. (B) Kv3 K^+ channels repolarize Ca^{2+} spikes, decrease Ca^{2+} spike amplitude and generate the subsequent fast AHP, and set the frequency of Ca^{2+} spike discharge. (C) Kv3 K^+ channels control the overall frequency of Ca–Na spike burst output (indirectly via the regulation of Ca^{2+} spikes and thus Ca^{2+}-dependent AHPs), and contribute to both the duration of the spike burst event and the frequency of Na^+ spikes within each burst.

subunit mRNA (Weiser *et al*., 1994). It may be that heteromeric expression of Kv3.3 and Kv3.4 subunits in Purkinje cells also leads to a leftward shift in voltage-dependence with respect to those recorded in heterologous expression systems.

Our finding DTX-sensitive current (Kv1.x K^+ channels) differs from the recordings of Southan & Robertson (2000), who reported no effect with DTX application in mouse Purkinje cells. These differences could arise from the specific recording conditions used or even reflect species or age differences, as suggested by a prominent TEA-insensitive and inactivating current in very young mouse Purkinje cells in the presence of 4 mM TEA (Sacco & Tempia, 2002). In our cells, 4 mM TEA blocked 86.2 ± 1.8% of current in the outside-out configuration, with no evidence of a residual inactivating current (data not shown; $n = 8$).

Previous voltage-clamp studies have identified substantial BK K^+ current in dissociated Purkinje cells (Raman & Bean, 1999; Womack & Khodakhah, 2002b; Swensen & Bean, 2003). In contrast, it has been difficult to identify the role of BK channels under current-clamp recording conditions without simultaneously blocking other ion channels (Edgerton & Reinhart, 2003; Womack & Khodakhah, 2004). Our attempts to use the selective BK blocker IBTX produced similar effects to CBTX, although much smaller in magnitude. This result likely reflects a change in IBTX sensitivity resulting from the presence of BK channel β subunits in Purkinje cells (Dworetzky *et al*., 1996; Chang *et al*., 1997). Although CBTX also blocks Kv1.3 channels, we verified that application of MGTX, another Kv1.3 blocker, did not reproduce the effects obtained with CBTX (Stuhmer *et al*., 1989; Coetzee et al., 1999). BK K^+ channels thus have an important role along with Kv3 channels in establishing Purkinje cell spike patterns (Fig. 7).

Na^+ spikes

Kv3 K^+ channels have been shown to repolarize Na^+ spikes to maintain high frequencies of discharge, a role consistent with their distribution in several high-frequency firing cells (Rudy & McBain, 2001). This is a property shared by Purkinje cells, which generate extremely short-duration spikes and have the capacity to discharge at frequencies up to 500 Hz. Previous work also established that TEA-sensitive K^+ channels are responsible for the majority of K^+ current involved in repolarizing Purkinje cell Na^+ spikes (Raman & Bean, 1999). Our work now indicates that these TEA-sensitive repolarizing currents are comprised primarily of the Kv3 class of K^+ channels. The importance of Kv3 channels to Na^+ spike repolarization was evident by a ∼25% decrease in the rate of repolarization and reduction of the fast AHP in only 150 μM TEA. The frequency of Na spike discharge was determined in part by Kv3 channels, but also included a contribution from Ca^{2+}-dependent K^+ channels.

Ca^{2+} spikes

The mixed Ca–Na spike response triggered by climbing fibre synaptic inputs in proximal dendrites of Purkinje cells has been shown to activate Kv3 currents when applied as a voltage-clamp command (Martina *et al*., 2003). We have extended these findings by demonstrating that Kv3 channels actively repolarize Purkinje cell Ca^{2+} spikes and Ca–Na spike bursts under physiological conditions. These actions have multiple consequences on how Ca^{2+} spikes regulate the final pattern and rate of Na^+ spike discharge. Blocking Kv3 K^+ channels slowed burst frequency on average by 45% over the entire range of current intensities, reducing the occurrence of Na^+ spike bursts propagated as an efferent signal. Additionally, blocking Kv3 channels increased the amplitude and duration of Ca^{2+} spikes to the point where Na^+ spike inactivation was substantially increased. In many cases this could block all Na^+ spike discharge for current injections greater than ∼3 nA. This result is particularly interesting with respect to the potential for dendritic Ca^{2+} spikes to contribute to signal processing in Purkinje cells, as the depolarization triggered by climbing fibre inputs also injects current in the order of ∼3 nA (Foster *et al*., 2002). Because both Kv3 and BK channels participated in the regulation of Ca^{2+} spike amplitude, we cannot rule out at this time that the exact role of Kv3 channels for this parameter was not slightly influenced by simultaneous block of the BK currents by TEA. Assuming that the properties of somatic Na^+ spikes are representative of those in the axon hillock region, these results indicate that full-blown Ca^{2+} spikes are normally held back by Kv3 activation, preventing undue Na^+ channel inactivation to ensure efficient burst output. Without Kv3 channels, Na^+ spike output would be altered by a decrease in both the frequency of burst discharge and the number of Na^+ spikes triggered per burst. This shift in input–output relations would translate to a decrease in the extent of inhibition of deep cerebellar nuclear neurons.

Acknowledgements

We gratefully acknowledge the technical assistance of M. Kruskic, A.J. Rashid and R.J. Dunn for providing Kv3.3b cDNA. This work was supported by the CIHR and an AHFMR Scientist Award to R.W.T. B.E.M. was supported by an AHFMR Studentship, NSERC Postgraduate Fellowship, CIHR Canada Graduate Scholarship and a Killam Trust Scholarship.

Abbreviations

4-AP, 4-aminopyridine; aCSF, artificial cerebrospinal fluid; BK, large-conductance Ca^{2+}-activated K^+ channels; CBTX, charybdotoxin; DTX, α-dendrotoxin; IBTX, iberiotoxin; MGTX, margatoxin; TEA, tetraethylammonium chloride; TTX, tetrodotoxin.

References

Baranauskas, G., Tkatch, T., Nagata, K., Yeh, J.Z. & Surmeier, D.J. (2003) Kv3.4 subunits enhance the repolarizing efficiency of Kv3.1 channels in fast-spiking neurons. *Nat. Neurosci.*, **6**, 258–266.

Brown, D.A. & Adams, P.R. (1980) Muscarinic suppression of a novel voltage-sensitive K+ current in a vertebrate neurone. *Nature*, **283**, 673–676.

Bushell, T., Clarke, C., Mathie, A. & Robertson, B. (2002) Pharmacological characterization of a non-inactivating outward current observed in mouse cerebellar Purkinje neurones. *Br. J. Pharmacol.*, **135**, 705–712.

Cavelier, P., Desplantez, T., Beekenkamp, H. & Bossu, J.L. (2003) K+ channel activation and low-threshold Ca2+ spike of rat cerebellar Purkinje cells in vitro. *Neuroreport*, **14**, 167–171.

Chang, C.P., Dworetzky, S.I., Wang, J. & Goldstein, M.E. (1997) Differential expression of the alpha and beta subunits of the large-conductance calcium-activated potassium channel: implication for channel diversity. *Brain Res. Mol. Brain Res.*, **45**, 33–40.

Chung, Y.H., Shin, C., Kim, M.J., Lee, B.K. & Cha, C.I. (2001) Immunohistochemical study on the distribution of six members of the Kv1 channel subunits in the rat cerebellum. *Brain Res.*, **895**, 173–177.

Cingolani, L.A., Gymnopoulos, M., Boccaccio, A., Stocker, M. & Pedarzani, P. (2002) Developmental regulation of small-conductance Ca2+-activated K+ channel expression and function in rat Purkinje neurons. *J. Neurosci.*, **22**, 4456–4467.

Coetzee, W.A., Amarillo, Y., Chiu, J., Chow, A., Lau, D., McCormack, T., Moreno, H., Nadal, M.S., Ozaita, A., Pountney, D., Saganich, M., Vega-Saenz de Miera, E. & Rudy, B. (1999) Molecular diversity of K+ channels. *Ann. N Y Acad. Sci.*, **868**, 233–285.

Devaux, J., Alcaraz, G., Grinspan, J., Bennett, V., Joho, R., Crest, M. & Scherer, S.S. (2003) Kv3.1b is a novel component of CNS nodes. *J. Neurosci.*, **23**, 4509–4518.

Dworetzky, S.I., Boissard, C.G., Lum-Ragan, J.T., McKay, M.C., Post-Munson, D.J., Trojnacki, J.T., Chang, C.P. & Gribkoff, V.K. (1996) Phenotypic alteration of a human BK (hSlo) channel by hSlobeta subunit coexpression: changes in blocker sensitivity, activation/relaxation and inactivation kinetics, and protein kinase A modulation. *J. Neurosci.*, **16**, 4543–4550.

Edgerton, J.R. & Reinhart, P.H. (2003) Distinct contributions of small and large conductance Ca2+-activated K+ channels to rat Purkinje neuron function. *J. Physiol. (Lond.)*, **548**, 53–69.

Erisir, A., Lau, D., Rudy, B. & Leonard, C.S. (1999) Function of specific K (+) channels in sustained high-frequency firing of fast-spiking neocortical interneurons. *J. Neurophysiol.*, **82**, 2476–2489.

Etzion, Y. & Grossman, Y. (1998) Potassium currents modulation of calcium spike firing in dendrites of cerebellar Purkinje cells. *Exp. Brain Res.*, **122**, 283–294.

Fernandez, F.R., Morales, E., Rashid, A.J., Dunn, R.J. & Turner, R.W. (2003) Inactivation of Kv3.3 potassium channels in heterologous expression systems. *J. Biol. Chem.*, **278**, 40890–40898.

Foster, K.A., Kreitzer, A.C. & Regehr, W.G. (2002) Interaction of postsynaptic receptor saturation with presynaptic mechanisms produces a reliable synapse. *Neuron*, **36**, 1115–1126.

Goldman-Wohl, D.S., Chan, E., Baird, D. & Heintz, N. (1994) Kv3.3b: a novel Shaw type potassium channel expressed in terminally differentiated cerebellar Purkinje cells and deep cerebellar nuclei. *J. Neurosci.*, **14**, 511–522.

Knaus, H.G., Schwarzer, C., Koch, R.O., Eberhart, A., Kaczorowski, G.J., Glossmann, H., Wunder, F., Pongs, O., Garcia, M.L. & Sperk, G. (1996) Distribution of high-conductance Ca(2+)-activated K+ channels in rat brain: targeting to axons and nerve terminals. *J. Neurosci.*, **16**, 955–963.

Latham, A. & Paul, D.H. (1971) Spontaneous activity of cerebellar Purkinje cells and their responses to impulses in climbing fibres. *J. Physiol. (Lond.)*, **213**, 135–156.

Lien, C.C. & Jonas, P. (2003) Kv3 potassium conductance is necessary and kinetically optimized for high-frequency action potential generation in hippocampal interneurons. *J. Neurosci.*, **23**, 2058–2068.

Llinas, R. & Sugimori, M. (1980a) Electrophysiological properties of in vitro Purkinje cell dendrites in mammalian cerebellar slices. *J. Physiol. (Lond.)*, **305**, 197–213.

Llinas, R. & Sugimori, M. (1980b) Electrophysiological properties of in vitro Purkinje cell somata in mammalian cerebellar slices. *J. Physiol. (Lond.)*, **305**, 171–195.

Martina, M., Schultz, J.H., Ehmke, H., Monyer, H. & Jonas, P. (1998) Functional and molecular differences between voltage-gated K+ channels of fast-spiking interneurons and pyramidal neurons of rat hippocampus. *J. Neurosci.*, **18**, 8111–8125.

Martina, M., Yao, G.L. & Bean, B.P. (2003) Properties and functional role of voltage-dependent potassium channels in dendrites of rat cerebellar Purkinje neurons. *J. Neurosci.*, **23**, 5698–5707.

Matsukawa, H., Wolf, A.M., Matsushita, S., Joho, R.H. & Knopfel, T. (2003) Motor dysfunction and altered synaptic transmission at the parallel fiber-Purkinje cell synapse in mice lacking potassium channels Kv3.1 and Kv3.3. *J. Neurosci.*, **23**, 7677–7684.

Midtgaard, J., Lasser-Ross, N. & Ross, W.N. (1993) Spatial distribution of Ca2+ influx in turtle Purkinje cell dendrites in vitro: role of a transient outward current. *J. Neurophysiol.*, **70**, 2455–2469.

Monsivais, P. & Hausser, M. (2003) Initiation and propagation of action potentials in axons of Purkinje neurons. *Int. Soc. Neurosci. Abstr.*, 476.473. [New Orleans 2003, Soc. Neuroscience, Washington D.C.]

Noonan, L., Doiron, B., Laing, C., Longtin, A. & Turner, R.W. (2003) A dynamic dendritic refractory period regulates burst discharge in the electrosensory lobe of weakly electric fish. *J. Neurosci.*, **23**, 1524–1534.

Pouille, F., Cavelier, P., Desplantez, T., Beekenkamp, H., Craig, P.J., Beattie, R.E., Volsen, S.G. & Bossu, J.L. (2000) Dendro-somatic distribution of calcium-mediated electrogenesis in purkinje cells from rat cerebellar slice cultures. *J. Physiol. (Lond.)*, **527**, 265–282.

Raman, I.M. & Bean, B.P. (1999) Ionic currents underlying spontaneous action potentials in isolated cerebellar Purkinje neurons. *J. Neurosci.*, **19**, 1663–1674.

Rashid, A.J., Dunn, R.J. & Turner, R.W. (2001a) A prominent soma-dendritic distribution of Kv3.3 K+ channels in electrosensory and cerebellar neurons. *J. Comp. Neurol.*, **441**, 234–247.

Rashid, A.J., Morales, E., Turner, R.W. & Dunn, R.J. (2001b) The contribution of dendritic Kv3 K+ channels to burst threshold in a sensory neuron. *J. Neurosci.*, **21**, 125–135.

Rudy, B., Chow, A., Lau, D., Amarillo, Y., Ozaita, A., Saganich, M., Moreno, H., Nadal, M.S., Hernandez-Pineda, R., Hernandez-Cruz, A., Erisir, A., Leonard, C. & Vega-Saenz de Miera, E. (1999) Contributions of Kv3 channels to neuronal excitability. *Ann. N Y Acad. Sci.*, **868**, 304–343.

Rudy, B. & McBain, C.J. (2001) Kv3 channels: voltage-gated K+ channels designed for high-frequency repetitive firing. *Trends Neurosci.*, **24**, 517–526.

Rudy, B., Sen, K., Vega-Saenz de Miera, E., Lau, D., Ried, T. & Ward, D.C. (1991) Cloning of a human cDNA expressing a high voltage-activating, TEA-sensitive, type-A K+ channel which maps to chromosome 1 band p21. *J. Neurosci. Res.*, **29**, 401–412.

Sacco, T. & Tempia, F. (2002) A-type potassium currents active at subthreshold potentials in mouse cerebellar Purkinje cells. *J. Physiol. (Lond.)*, **543**, 505–520.

Saganich, M.J., Machado, E. & Rudy, B. (2001) Differential expression of genes encoding subthreshold-operating voltage-gated K+ channels in brain. *J. Neurosci.*, **21**, 4609–4624.

Sekirnjak, C., Martone, M.E., Weiser, M., Deerinck, T., Bueno, E., Rudy, B. & Ellisman, M. (1997) Subcellular localization of the K+ channel subunit Kv3.1b in selected rat CNS neurons. *Brain Res.*, **766**, 173–187.

Seo, W.S., Shin, J.H. & Suh, C.K. (1999) 4-Aminopyridine (4-AP) augments Ca (2+)-dependent action potential and changes oscillatory firing patterns in rat cerebellar Purkinje cells. *Yonsei Med. J.*, **40**, 112–117.

Southan, A.P. & Robertson, B. (2000) Electrophysiological characterization of voltage-gated K (+) currents in cerebellar basket and purkinje cells: Kv1 and Kv3 channel subfamilies are present in basket cell nerve terminals. *J. Neurosci.*, **20**, 114–122.

Stuart, G.J., Dodt, H.U. & Sakmann, B. (1993) Patch-clamp recordings from the soma and dendrites of neurons in brain slices using infrared video microscopy. *Pflugers Arch.*, **423**, 511–518.

Stuart, G. & Hausser, M. (1994) Initiation and spread of sodium action potentials in cerebellar Purkinje cells. *Neuron*, **13**, 703–712.

Stuhmer, W., Ruppersberg, J.P., Schroter, K.H., Sakmann, B., Stocker, M., Giese, K.P., Perschke, A., Baumann, A. & Pongs, O. (1989) Molecular basis of functional diversity of voltage-gated potassium channels in mammalian brain. *EMBO J.*, **8**, 3235–3244.

Swensen, A.M. & Bean, B.P. (2003) Ionic mechanisms of burst firing in dissociated Purkinje neurons. *J. Neurosci.*, **23**, 9650–9663.

Telgkamp, P. & Raman, I.M. (2002) Depression of inhibitory synaptic transmission between Purkinje cells and neurons of the cerebellar nuclei. *J. Neurosci.*, **22**, 8447–8457.

Vega-Saenz de Miera, E., Moreno, H., Fruhling, D., Kentros, C. & Rudy, B. (1992) Cloning of ShIII (Shaw-like) cDNAs encoding a novel high voltage-activating, TEA sensitive, type-A K+ channel. *Proc. R. Soc. Lond. B*, **248**, 9–18.

Veh, R.W., Lichtinghagen, R., Sewing, S., Wunder, F., Grumbach, I.M. & Pongs, O. (1995) Immunohistochemical localization of five members of the Kv1 channel subunits: contrasting subcellular locations and neuron-specific co-localizations in rat brain. *Eur. J. Neurosci.*, **7**, 2189–2205.

Wang, L.Y., Gan, L., Forsythe, I.D. & Kaczmarek, L.K. (1998b) Contribution of the Kv3.1 potassium channel to high-frequency firing in mouse auditory neurones. *J. Physiol. (Lond.)*, **509**, 183–194.

Wang, H.S., Pan, Z., Shi, W., Brown, B.S., Wymore, R.S., Cohen, I.S., Dixon, J.E. & McKinnon, D. (1998a) KCNQ2 and KCNQ3 potassium channel subunits: molecular correlates of the M-channel. *Science*, **282**, 1890–1893.

Weiser, M., Vega-Saenz de Miera, E., Kentros, C., Moreno, H., Franzen, L., Hillman, D., Baker, H. & Rudy, B. (1994) Differential expression of Shaw-related K^+ channels in the rat central nervous system. *J. Neurosci.*, **14**, 949–972.

Womack, M. & Khodakhah, K. (2002a) Active contribution of dendrites to the tonic and trimodal patterns of activity in cerebellar Purkinje neurons. *J. Neurosci.*, **22**, 10603–10612.

Womack, M.D. & Khodakhah, K. (2002b) Characterization of large conductance Ca2+-activated K+ channels in cerebellar Purkinje neurons. *Eur. J. Neurosci.*, **16**, 1214–1222.

Womack, M.D. & Khodakhah, K. (2003) Somatic and dendritic small-conductance calcium-activated potassium channels regulate the output of cerebellar purkinje neurons. *J. Neurosci.*, **23**, 2600–2607.

Womack, M.D. & Khodakhah, K. (2004) Dendritic control of spontaneous bursting in cerebellar Purkinje cells. *J. Neurosci.*, **24**, 3511–3521.